m_j-Resolved Doppler Spectroscopy of $Cs(6p^2P_{\frac{3}{2},m_j})$ Atoms Predissociated from a Single Level $Cs_2D^1\Sigma_u^+$ (v=46, J=54)

Kensuke Matsubara,* Yumi Tajima, Masaaki Baba,# Jun Kawai, and Hajime Katô*

Department of Chemistry, Faculty of Science, Kobe University, Nada-ku, Kobe 657

(Received June 10, 1996)

In a plane perpendicular to a magnetic field a collimated cesium beam was crossed at right angles by a pump laser beam. Cs_2 molecules were excited to the $D^1\Sigma_u^+$ ($v=46$, $J=54$) level, which predissociated selectively to $Cs(6s^2S_{\frac{1}{2}})$ + $Cs(6p^2P_{\frac{3}{2}})$ atoms. The m_j-resolved excitation spectra of the $Cs(8s^2S_{\frac{1}{2},m_j'} \leftarrow 6p^2P_{\frac{3}{2},m_j})$ transitions at a magnetic field of 1.91 kG were measured using a probe laser beam propagated either along the magnetic field or along the pump beam. The population of $Cs(6p^2P_{\frac{3}{2},m_j})$ atoms was found to be in the ratio 77 : 136 : 100 : 46 for $m_j = \frac{3}{2}$, $\frac{1}{2}$, $-\frac{1}{2}$, and $-\frac{3}{2}$ based on an analysis of the line intensities. From the line shapes of the excitation spectra, $Cs(6p^2P_{\frac{3}{2},\pm\frac{1}{2}})$ atoms were found to recoil predominantly parallel to the magnetic field $\boldsymbol{H}$, and $Cs(6p^2P_{\frac{3}{2},\pm\frac{3}{2}})$ atoms were found to recoil predominantly perpendicular to $\boldsymbol{H}$.

From the excitation spectra of the photofragments we can obtain information about the distribution of the recoil velocity vector and the orientation of the fragments in addition to the rotational, vibrational, and electronic state distributions. With the development of lasers, the spatial distribution of the velocity vectors of photofragments has been studied by the Doppler line shape of the excitation spectrum, and by its dependence on the directions of the polarization and propagation of the probe laser beam.[1,2] The Doppler line shape of the atomic fluorescence, following the photodissociation of a diatomic molecule, was formulated by studying the correlation between the transition dipole moment of the parent molecule and the anisotropic distribution of the recoil velocity vector of the atomic fragments.[3] The degree of polarization of the atomic fluorescence was related to the anisotropy in the angular distribution.[4] The transition moment of the atomic fragment depends on the total angular momentum quantum number j and the component m_j along the space-fixed Z axis. If an external magnetic field is applied along the Z axis, the m_j components can be separated by the Zeeman splitting. We shall report on the m_j dependence of the Doppler line shape and intensity of the excitation spectrum of the photodissociated atoms. These are fundamental and important physical quantities for understanding the dynamics of the photodissociation; this is the first report concerning the m_j-resolved Doppler line shape, as far as the authors know.

When a discrete state B, which predissociates, and another discrete state A can interact, some levels of A, which are accidentally close in energy with B and have a significant interaction with B, are observed to predissociate. This phenomenon is called *indirect* (or *accidental*) *predissociation*.[5] In such cases a single predissociative level can be selectively excited with narrow-linewidth laser light, and one can then study the dissociation from a chosen electronic-vibrational-rotational level. The $D^1\Sigma_u^+$ state of the Cs_2 molecule was found to dissociate selectively to the separated atoms $Cs(6p^2P_{\frac{3}{2}})$ + $Cs(6s^2S_{\frac{1}{2}})$,[6] and the line broadening and the vibrational level shifts were observed in some of the transition lines.[7,8] This dissociation was extensively studied, and could be attributed to indirect predissociation caused by the spin–orbit interaction between discrete levels, $D^1\Sigma_u^+$ (vJ) and $(2)^3\Pi_{0u}$ ($v'J$), and the L-uncoupling interaction between the discrete level $(2)^3\Pi_{0u}$ ($v'J$) and the dissociative continuum $c^3\Sigma_u^+$ (v_cN).[9] When an external magnetic field was applied, a shortening of the lifetime was observed for the $D^1\Sigma_u^+$ ($v=27$ and 47, J) levels.[10] A variation in the linewidth with the strength of the magnetic field H was observed for a number of transition lines.[11]

The $Cs_2D^1\Sigma_u^+$ ($v=46$, $J=54$) $\leftarrow X^1\Sigma_g^+$ ($v=0$, $J=55$) transition was chosen as a pump transition, because the line was isolated from other transition lines and the effect of the magnetic field had been well studied.[11] When a molecular beam of cesium was excited to the $D^1\Sigma_u^+$ ($v=46$, $J=54$) level, a strong emission of the $Cs(6p^2P_{\frac{3}{2}} \rightarrow 6s^2S_{\frac{1}{2}})$ transition was observed as a result of dissociation to $Cs(6p^2P_{\frac{3}{2}})$+$Cs(6s^2S_{\frac{1}{2}})$ atoms. $Cs(6s^2S_{\frac{1}{2}})$ atoms coexist within a molecular beam of cesium; the ratio of Cs to Cs_2 is about 10^2. Therefore, we could not measure the excitation spectrum of the dissociation product $Cs(6s^2S_{\frac{1}{2}})$ separately. We shall study the m_j dependence of the population and the Doppler profile of the

Present address: Faculty of Integrated Human Studies, Kyoto University, Sakyo-ku, Kyoto 606.

dissociation products $Cs(6p^2P_{\frac{3}{2},m_j})$ by measuring the excitation spectrum of the $Cs(8s^2S_{\frac{1}{2},m_j'} \leftarrow 6p^2P_{\frac{3}{2},m_j})$ transition in a magnetic field.

Experimental

The scheme for measurement of the m_j-resolved excitation spectrum is shown in Fig. 1. In a magnetic field, the excitation spectrum of Cs_2 was measured by scanning the wavenumber of the pump laser; the wavenumber of the pump laser was then fixed to the center of a line of the $D^1\Sigma_u^+$ ($v=46$, $J=54$) $\leftarrow$ $X^1\Sigma_g^+$ ($v=0$, J=55) transition. In this case only one atomic emission of the $Cs(6p^2P_{\frac{3}{2}} \rightarrow 6s^2S_{\frac{1}{2}})$ transition was observed in addition to the molecular fluorescence $D^1\Sigma_u^+$ ($v=46$, $J=54$) $\rightarrow$ $X^1\Sigma_g^+$ (v'',$J=55$ and 53). We scanned the wavenumber of the probe laser around the region of the $Cs(8s^2S_{\frac{1}{2}} \leftarrow 6p^2P_{\frac{3}{2}})$ transition at 12584.82 cm^{-1} while measuring the emission intensity of the $Cs(8s^2S_{\frac{1}{2}} \rightarrow 6p^2P_{\frac{1}{2}})$ transition at 13138.93 cm^{-1}. The excitation spectrum of each m_j component of the dissociation product $Cs(6p^2P_{\frac{3}{2},m_j})$ could be measured separately in a magnetic field of 1.91 kG.

A collimated cesium beam was crossed at right angles by the pump laser beam, and the electric vector of the pump beam was set at right angles to the propagation vector of the cesium beam. An external magnetic field $\boldsymbol{H}$ was applied parallel to the electric vector of the pump beam: π-polarization. The apparatus is shown schematically in Fig. 2. The probe laser beam was propagated either parallel to $\boldsymbol{H}$ (passed through the holes at the center of the pole pieces, as shown in Fig. 2(b)) or parallel and in the opposite direction to the propagation vector of the pump laser beam (the electric vector of the probe laser beam was perpendicular to $\boldsymbol{H}$: σ-polarization). The magnetic field was generated by an electromagnet, whose coils were located outside of a chamber, and the pole pieces were extended to inside of the chamber shielded by O rings. The pole pieces were 55 mm diameter and tapered to 25 mm diameter, and a hole of 5 mm diameter was located at the center. The magnitude of the magnetic field was measured by a Gauss meter; a maximum of 2.4 kG could be obtained at a separation of 70 mm. The cesium beam was generated by an oven cell, which contained cesium metal (99.9% purity) and was kept at 600 K, equipped with an orifice of 300 μm in a high vacuum chamber ($<10^{-6}$ Torr, 1

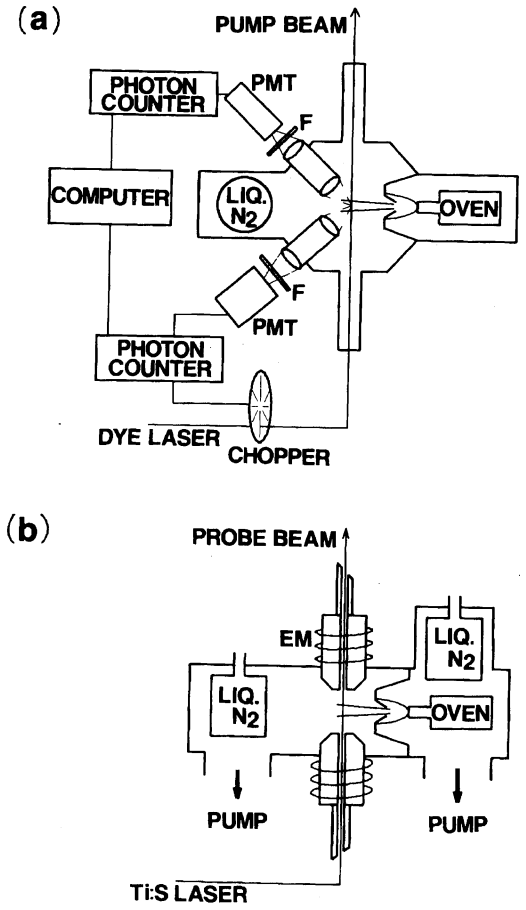

Fig. 2. A schematic diagram of our experimental setup. (a) is the over view and (b) is the side view. The probe laser beam is propagated parallel to the magnetic field in this setup. In another setup, the probe laser beam is propagated parallel and opposite (anti-parallel) to the propagation vector of the pump laser beam. EM, PMT, and F represent, respectively, an electric magnet, a photomultiplier, and an optical bandpass filter.

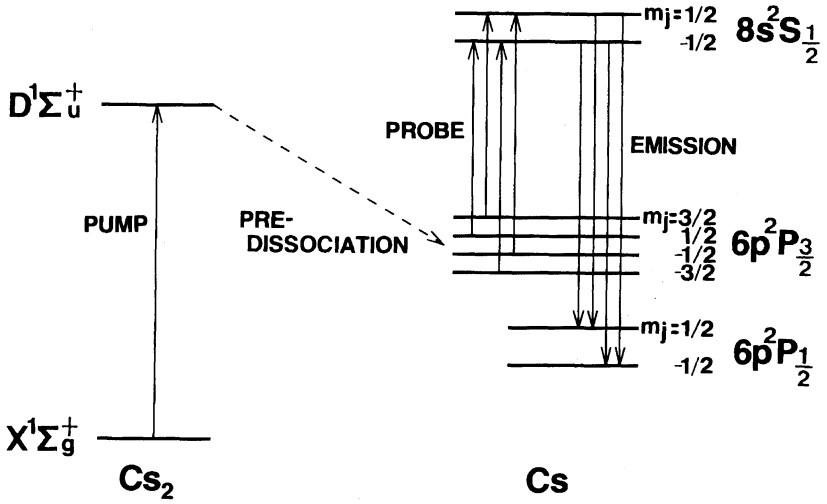

Fig. 1. The scheme of measurement of m_j-resolved excitation spectrum of the $Cs(6p^2P_{\frac{3}{2},m_j})$ atoms predissociated from the $Cs_2D^1\Sigma_u^+$ ($v=46$, $J=54$) level.

Torr = 133.322 Pa). The cesium beam was collimated by a conical skimmer having an inner diameter of 1 mm and crossed with the laser beam at the center of the magnetic field. The distance between the nozzle and skimmer was 10 mm, and the distance between the skimmer and the crossing point was 30 mm. The cesium beam was trapped by a liquid-nitrogen trap set.

A single-mode tunable dye laser (Coherent 699-29, linewidth 500 kHz) with R6G dye was used as the pump laser, and a single-mode tunable Ti : Sapphire laser (Coherent 899-29, linewidth 500 kHz) was used as the probe laser. The diameters of the pump and probe laser beams were both 1 mm at the sampling point. The $Cs(8s^2S_{\frac{1}{2}} \rightarrow 6p^2P_{\frac{1}{2}})$ emission was collected by lenses through a bandpass filter which transmitted light between 759 and 763 nm, and was detected by a photomultiplier (Hamamatsu R943-02). The photocurrent was amplified and counted by a photon counter (Hamamatsu C767). While scanning the probe laser around 12584.82 cm^{-1}, we found that the $A^1\Sigma_u^+ \leftarrow X^1\Sigma_g^+$ transition was also induced and the resulting fluorescence had an intensity around 761 nm. The initial level of the A $\leftarrow$ X transition was not $X^1\Sigma_g^+$ ($v=0$, $J=55$). We modulated the pump beam by a chopper synchronized with the photon counter, and measured the difference between the photon number counted when both the pump and the probe beams were incident and the one counted when only the probe beam was incident. We could thus remove the effects of obstractive emission, because the emission intensity originating from the $A^1\Sigma_u^+ \leftarrow X^1\Sigma_g^+$ transition was independent of the pump transition $D^1\Sigma_u^+$ ($v=46$, $J=54$) $\leftarrow X^1\Sigma_g^+$ ($v=0$, $J=55$). In order to check the stability of the excitation, we monitored the intensity of the $6p^2P_{\frac{3}{2}} \rightarrow 6s^2S_{\frac{1}{2}}$ emission (the D_2 line) during a measurement of the excitaion spectrum. This was collected by another set of lenses through a bandpass filter, which transmitted light between 847 to 857 nm, and was detected by a photomultiplier (RCA C31034). The photocurrent was amplified and counted by a photon counter (EG&G PARC Model 1109 and 1191). These data were processed by a computer (NEC 9801). By confirming that the intensity of the D_2 line was linear to the power of the pump laser beam and that the intensity of the excitation spectrum of the $Cs(6p^2P_{\frac{3}{2},m_j})$ atoms was linear to the power of the probe laser beam, we removed the effects of laser power saturation.

The m_j-resolved excitation spectrum of the $Cs(8s^2S_{\frac{1}{2},m_j'} \leftarrow 6p^2P_{\frac{3}{2},m_j})$ transition observed by the probe beam propagated parallel to $\boldsymbol{H}$ is shown in Fig. 3. The excitation spectrum observed by the probe beam propagated anti-parallel to the pump beam is shown in Fig. 4. Considerable differences are observed in both the line intensity and the line shape. We shall discuss these observed results below.

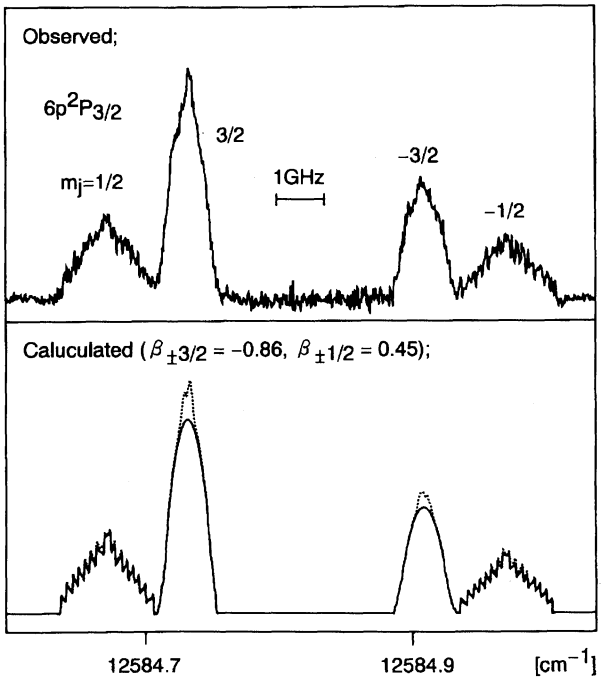

Fig. 3. Upper trace is the excitation spectrum of the $Cs(6p^2P_{\frac{3}{2},m_j})$ atoms at $H=1.91$ kG observed by the probe laser beam propagated parallel to the magnetic field, where the electric vector of the probe beam was perpendicular to the magnetic field : σ-polarization. The assignments of m_j are indicated for each line. In the lower trace, a broken line is the simulated excitation spectrum including effects of the self-absorption. A solid line is the simulated excitation spectrum without the self-absorption.

Theoretical

1. Splitting and Intensity of the $Cs(8s^2S_{\frac{1}{2},m_j'} \leftarrow 6p^2P_{\frac{3}{2},m_j})$ Transition. In order to analyze the excitation spectra of the $Cs(8s^2S_{\frac{1}{2},m_j'} \leftarrow 6p^2P_{\frac{3}{2},m_j})$ transitions, let us calculate the energy splittings and the line intensities. The ^{133}Cs atom has a nuclear spin of $I=7/2$. The magnetic hyperfine constant A_J is reported to be 50.31 MHz for the $6p^2P_{\frac{3}{2}}$ state and 218.88 MHz for the $8s^2S_{\frac{1}{2}}$ state, and the electric quadrupole interaction constant B_J is reported to be −0.38 MHz for the $6p^2P_{\frac{3}{2}}$ state and zero for the $8s^2S_{\frac{1}{2}}$ state.[12] Let us express the total angular momentum of an atom as $\boldsymbol{F}=\boldsymbol{j}+\boldsymbol{I}$, where $\boldsymbol{j}$ is the sum of the orbital angular momentum $\boldsymbol{L}$ and the spin angular momentum $\boldsymbol{S}$ of electrons, and $\boldsymbol{I}$ is the nuclear spin angular momentum. For the basis function $|LSjIFM_F>$, the nonvanishing matrix elements of the hyperfine interaction H_{hfs} are given by[12,13]

$$<LSjIFm_F|H_{hfs}|LSjIFm_F> = \frac{A_J}{2}[FIj] + \frac{B_J}{2I(2I-1)2j(2j-1)}\left\{\frac{3}{2}[FIj]([FIj]+1) - 2I(I+1)j(j+1)\right\}, \quad (1)$$

where $[FIj]=F(F+1)-I(I+1)-j(j+1)$. If we neglect the magnetic moment originating from the nuclear spin, which is much smaller than that of the electrons, the matrix elements of the Zeeman interaction H_Z are given by[14]

$$< LSjIF'm_F'|H_Z|LSjIFm_F > = \mu_B H \sum_{m_I,m_j}\sum_{m_L,m_S} < Im_Ijm_j|F'm_F' >< Im_Ijm_j|Fm_F > \delta_{m_F,m_F'} \times < Lm_LSm_S|jm_j >< Lm_LSm_S|jm_j > (m_L+2m_S), \quad (2)$$

where m_L, m_S, m_j, and m_I are, respectively, the projections of $\boldsymbol{L}$, $\boldsymbol{S}$, $\boldsymbol{j}$, and $\boldsymbol{I}$ on the Z axis, and $<j_1j_2m_1m_2|j_3m_3>$ is the Clebsch–Gordan coefficients.

For excitation by light polarized along the space-fixed X axis, the nonvanishing transition moments are expressed as[14]

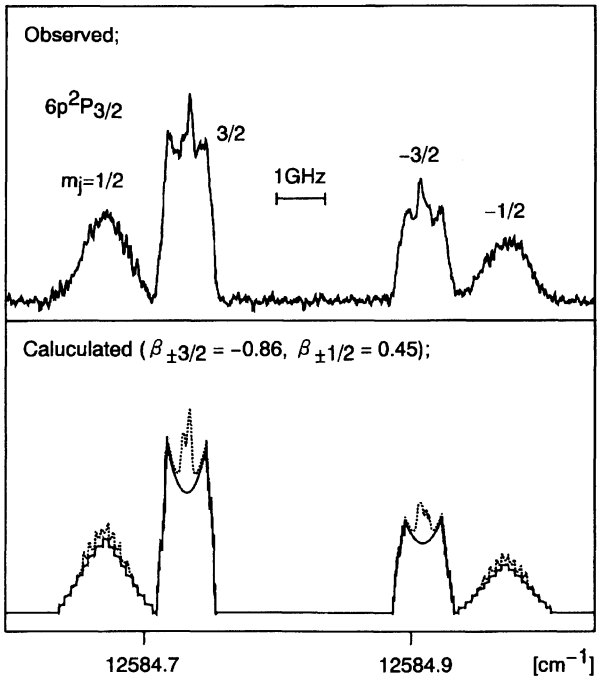

Fig. 4. Upper trace is the excitation spectrum of the $Cs(6p^2P_{\frac{3}{2},m_j})$ atoms at $H=1.91$ kG observed by the probe laser beam propagated anti-parallel to the pump beam, where the electric vector of the probe beam was perpendicular to the magnetic field: σ-polarization. The assignments of m_j are indicated for each line. In the lower trace, a broken line is the simulated excitation spectrum including effects of the self-absorption. A solid line is the simulated excitation spectrum without the self-absorption.

$$< 8s^2S_{\frac{1}{2}} F' m'_F|\mu_X|6p^2P_{\frac{3}{2}} F m_F > = \sum_{m_I,m_j} < \frac{1}{2} m_j \pm 1 \frac{7}{2} m_I|F' m'_F >< \frac{3}{2} m_j \frac{7}{2} m_I|F m_F > \times(\pm)\mu \frac{1}{2}\sqrt{\left(\frac{3}{2} \mp m_j\right)\left(\frac{1}{2} \mp m_j\right)}, \quad (3)$$

where μ is the electric dipole transition moment.

For the basis functions of $|6p^2P_{\frac{3}{2}}\ F m_F >$ and $|8s^2S_{\frac{1}{2}}\ F m_F >$ we calculated the eigenfunctions and eigenvalues of the Hamiltonian $H_{hfs}+H_Z$ for a magnetic field of $H=1.91$ kG by solving a secular equation composed of the matrix elements given by Eqs. 1 and 2; the resulting eigenenergies are shown schematically in Fig. 5. For the eigenfunctions we calculated the transition moments. The vertical lines in Fig. 5(a) show the allowed transitions in order of increasing transition energy from the left to the right. If we assume that all levels of the $6p^2P_{\frac{3}{2}}$ are equally populated, the line intensity is proportional to the square of the transition moment. The transition probability is shown by the length of the bars in Fig. 5(b). At $H=1.91$ kG, the Zeeman splitting is much larger than the hyperfine splitting, and the transitions can be grouped to the $8s^2S_{\frac{1}{2},-\frac{1}{2}} \leftarrow 6p^2P_{\frac{3}{2},\frac{1}{2}}$, $8s^2S_{\frac{1}{2},\frac{1}{2}} \leftarrow 6p^2P_{\frac{3}{2},\frac{3}{2}}$, $8s^2S_{\frac{1}{2},-\frac{1}{2}} \leftarrow 6p^2P_{\frac{3}{2},-\frac{3}{2}}$, and $8s^2S_{\frac{1}{2},\frac{1}{2}} \leftarrow 6p^2P_{\frac{3}{2},-\frac{1}{2}}$ transitions. The ratio of the transition probabilities is calculated to be 1 : 3 : 3 : 1, which is coincident with that in the absence of the hyperfine interaction.[14]

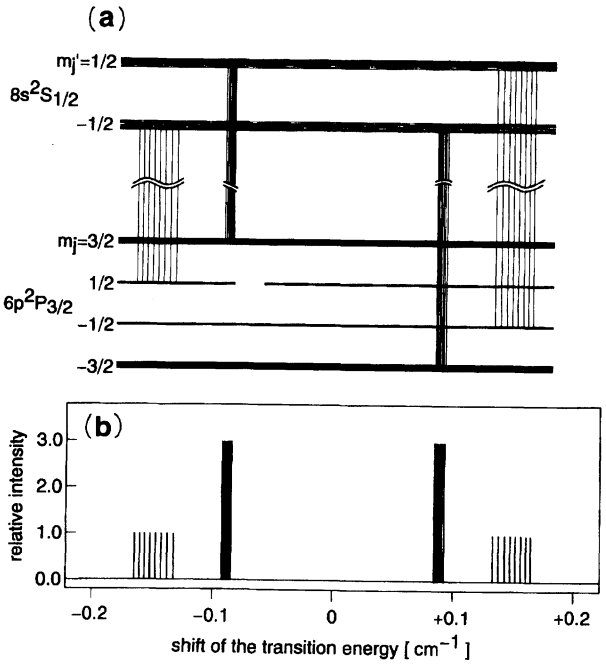

Fig. 5. (a) The level splitting of the $8s^2S_{\frac{1}{2}}$ and $6p^2P_{\frac{3}{2}}$ states caused by the hyperfine interaction and the Zeeman interaction at $H=1.91$ kG. The vertical lines show the allowed transitions by the σ-polarization, and the transition energy increases from the left to the right. (b) A square of the transition moment of each allowed transition is shown by the length of a vertical line, which is plotted against the energy shift.

2. Population on Magnetic Sublevels of the Predissociated Atoms. The predissociation of the $D^1\Sigma_u^+$ (vJ) levels was shown to occur through a combination of the spin–orbit interaction between the $D^1\Sigma_u^+$ (vJ) and $(2)^3\Pi_{0u}(ev'J)$ levels and the L-uncoupling interaction between the $(2)^3\Pi_{0u}$ $(ev'J)$ and $c^3\Sigma_u^+$ $(v_cN{=}JJ)$ levels.[9] The potential curve of the $c^3\Sigma_u^+$ state is repulsive, and decomposes into $Cs(6p^2P_{\frac{3}{2}})$ and $Cs(6s^2S_{\frac{1}{2}})$ atoms. The nonvanishing matrix elements of the spin–orbit interaction H_{SO} between the $D^1\Sigma_u^+$ (vJ) and $(2)^3\Pi_{0u}(ev'J)$ levels are[9]

$$<^1\Sigma_u^+ vJM|H_{SO}|^3\Pi_{0u} ev'JM >= \zeta, \quad (4)$$

where ζ is the spin–orbit coupling constant. The nonvanishing matrix elements of the L-uncoupling interaction H_{JL} between the $(2)^3\Pi_{0u}(ev'J)$ and $c^3\Sigma_u^+(v_cNJ)$ levels are[9]

$$<^3\Pi_{0u} ev'JM|H_{JL}|^3\Sigma_u^+ v_cN = JJM >= \sqrt{J(J+1)}B_L, \quad (5)$$

where $B_L{=}<v|\frac{\hbar^2}{2\mu R^2}<1|L_+|0^+>|v_c>$ is the L-uncoupling constant.

The effects of an external magnetic field on the predissociation were also studied in detail.[10,11] If we neglect small energies due to the spin-spin interaction and the spin-rotation interaction, the $^3\Sigma_u^+$ $(vN{=}JJ:F_2)$, $^3\Sigma_u^+(vN{=}JJ{+}1:F_1)$, and $^3\Sigma_u^+(vN{=}JJ-1:F_3)$ levels are degenerate. The eigenfunctions of a $^3\Sigma_u^+$ state in the presence of a magnetic field are[15,16]

$$|^3\Sigma_u^+ vN{=}JME_Z{=}2\mu_B H{>}{=}\sqrt{\frac{(J{+}M)(J{+}M{+}1)}{2(J{+}1)(2J{+}1)}}|^3\Sigma_u^+ vN{=}JJ{+}1M{>}$$
$$+\sqrt{\frac{(J{+}M)(J{-}M{+}1)}{2J(J{+}1)}}|^3\Sigma_u^+ vN{=}JJM{>}$$
$$+\sqrt{\frac{(J{-}M)(J{-}M{+}1)}{2J(2J{+}1)}}|^3\Sigma_u^+ vN{=}JJ{-}1M{>},$$
$$|^3\Sigma_u^+ vN{=}JME_Z{=}0{>}{=}-\sqrt{\frac{(J{+}M{+}1)(J{-}M{+}1)}{(J{+}1)(2J{+}1)}}|^3\Sigma_u^+ vN{=}JJ{+}1M{>}$$
$$+\frac{M}{\sqrt{J(J{+}1)}}|^3\Sigma_u^+ vN{=}JJM{>}$$
$$+\sqrt{\frac{(J{+}M)(J{-}M)}{J(2J{+}1)}}|^3\Sigma_u^+ vN{=}JJ{-}1M{>},$$
$$|^3\Sigma_u^+ vN{=}JME_Z{=}{-}2\mu_B H{>}{=}{-}\sqrt{\frac{(J{-}M{+}1)(J{-}M)}{2(J{+}1)(2J{+}1)}}|^3\Sigma_u^+ vN{=}JJ{+}1M{>}$$
$$+\sqrt{\frac{(J{-}M)(J{+}M{+}1)}{2J(2J{+}1)}}|^3\Sigma_u^+ vN{=}JJM{>}$$
$$-\sqrt{\frac{(J{+}M)(J{+}M{+}1)}{2J(2J{+}1)}}|^3\Sigma_u^+ vN{=}JJ{-}1M{>}, \quad (6)$$

and the eigenenergies are, respectively, $E_{ev}+B_vN(N+1)+2\mu_BH$, $E_{ev}+B_vN(N+1)$, and $E_{ev}+B_vN(N+1)-2\mu_BH$, where E_{ev} is the vibrational-electronic energy, B_v is the rotational constant, μ_B is the Bohr magneton, and H is the magnetic field. The nonvanishing matrix elements of the Zeeman interaction H_Z between the $(2)^3\Pi_{0u}(ev'J)$ and $c^3\Sigma_u^+(v_cNJ)$ levels are given in Ref. 11.

The nonvanishing matrix elements of $H_{JL}+H_Z$ between the $(2)^3\Pi_{0u}(ev'J)$ and $c^3\Sigma_u^+(v_cNE_Z)$ levels are calculated from Eq. 15 of Ref. 11, Eq. 5, and Eq. 6 as

$$<{}^3\Pi_{0u}ev'JM|H_{JL}+H_Z|{}^3\Sigma_u^+ v_cN=J+2ME_Z=2\mu_BH>$$
$$=\frac{1}{2(2J+3)}\sqrt{\frac{(J+M+1)(J-M+1)(J-M+2)(J-M+3)}{(2J+1)(2J+5)}}CH,$$
$$<{}^3\Pi_{0u}ev'JM|H_{JL}+H_Z|{}^3\Sigma_u^+ v_cN=J+2ME_Z=0>$$
$$=\frac{1}{2J+3}\sqrt{\frac{(J+M+1)(J+M+2)(J-M+1)(J-M+2)}{2(2J+1)(2J+5)}}CH,$$
$$<{}^3\Pi_{0u}ev'JM|H_{JL}+H_Z|{}^3\Sigma_u^+ v_cN=J+2ME_Z=-2\mu_BH>$$
$$=-\frac{1}{2(2J+3)}\sqrt{\frac{(J+M+1)(J+M+2)(J+M+3)(J-M+1)}{(2J+1)(2J+5)}}CH,$$
$$<{}^3\Pi_{0u}ev'JM|H_{JL}+H_Z|{}^3\Sigma_u^+ v_cN=JME_Z=2\mu_BH>$$
$$=\sqrt{(J+M)(J-M+1)}\left\{\frac{1}{\sqrt{2}}B_L-\frac{2M-1}{2(2J-1)(2J+3)}CH\right\},$$
$$<{}^3\Pi_{0u}ev'JM|H_{JL}+H_Z|{}^3\Sigma_u^+ v_cN=JME_Z=0>$$
$$=MB_L+\frac{\sqrt{2}(1-J-J^2-M^2)}{(2J-1)(2J+3)}CH,$$
$$<{}^3\Pi_{0u}ev'JM|H_{JL}+H_Z|{}^3\Sigma_u^+ v_cN=JME_Z=-2\mu_BH>$$
$$=\sqrt{(J-M)(J+M+1)}\left\{\frac{1}{\sqrt{2}}B_L-\frac{2M+1}{2(2J-1)(2J+3)}CH\right\},$$
$$<{}^3\Pi_{0u}ev'JM|H_{JL}+H_Z|{}^3\Sigma_u^+ v_cN=J-2ME_Z=2\mu_BH>$$
$$=-\frac{1}{2(2J-1)}\sqrt{\frac{(J-M)(J+M)(J+M-1)(J+M-2)}{(2J+1)(2J-3)}}CH,$$
$$<{}^3\Pi_{0u}ev'JM|H_{JL}+H_Z|{}^3\Sigma_u^+ v_cN=J-2ME_Z=0>$$
$$=\frac{1}{2J-1}\sqrt{\frac{(J-M)(J+M)(J+M-1)(J-M-1)}{2(2J+1)(2J-3)}}CH,$$
$$<{}^3\Pi_{0u}ev'JM|H_{JL}+H_Z|{}^3\Sigma_u^+ v_cN=J-2ME_Z=-2\mu_BH>$$
$$=\frac{1}{2(2J-1)}\sqrt{\frac{(J+M)(J-M)(J-M-1)(J-M-2)}{(2J+1)(2J-3)}}CH, \quad (7)$$

where $C=2^{-1/2}<v'|<1|L_+|0^+>|v_c>\mu_B$.

The rules for determining what type of atomic states result from the dissociation of a given molecular electronic state were derived by Wigner and Witmer,[17] and worked out by Mulliken.[18] Singer, Freed, and Band[19] studied the photodissociation of diatomic molecules by considering the conservation of the angular momenta, including the rotational angular momentum. By extending the theory given in Ref. 19, Katô and Onomichi[15] calculated the probability of producing a $Cs(6p^2P_{\frac{3}{2},m_j})$ atom by dissociation from the $c^3\Sigma_u^+(v_cN{=}JME_Z{=}0$ and $\pm2\mu_BH)$ levels. The probability is denoted by the symbol $MA[^3\Sigma_u^+(v_cN{=}JME_Z)\rightarrow 6p^2P_{\frac{3}{2},m_j}]$ and the algebraic formulas are listed in Table 1 of Ref. 15.

For excitation by plane-polarized light with its electric vector along the space-fixed Z axis, the nonvanishing transition moment for the P branch of the $^1\Sigma_u^+ \leftarrow {}^1\Sigma_g^+$ transition is given by[10]

$$<{}^1\Sigma_g^+ v''J{+}1M|\mu_Z|{}^1\Sigma_u^+ vJM{>}{=}\mu_{\|}\sqrt{\frac{(J{+}M{+}1)(J{-}M{+}1)}{(2J{+}1)(2J{+}3)}}, \quad (8)$$

where $\mu_{\|}$ is the electronic transition moment along the molecular axis.

The probability of producing a $Cs(6p^2P_{\frac{3}{2},m_j})$ atom via the molecular states $(2)^3\Pi_{0u}(ev'JM)$ and $c^3\Sigma_u^+(v_cN{=}J$ or $J{\pm}2ME_Z)$ following the excitation $D^1\Sigma_u^+(vJM)\leftarrow X^1\Sigma_g^+(v''J{+}1M)$ is proportional to the following factor:

$$|<{}^1\Sigma_g^+ v''J{+}1M|\mu_Z|{}^1\Sigma_u^+ vJM>|^2|<{}^1\Sigma_u^+ vJM|H_{SO}|{}^3\Pi_{0u}ev'JM>|^2$$
$$\times|<{}^3\Pi_{0u}ev'JM|H_{JL}+H_Z|{}^3\Sigma_u^+ v_cN{=}J\text{or}J\pm2ME_Z>|^2$$
$$\times MA[{}^3\Sigma_u^+(v_cN{=}J\text{or}J\pm2ME_Z)\rightarrow 6p^2P_{\frac{3}{2},m_j}]. \quad (9)$$

Let us express this factor as $P[^1\Sigma_g^+(v''J+1M)-{}^1\Sigma_u^+(vJM)-{}^3\Pi_{0u}(ev'JM)-{}^3\Sigma_u^+(v_cN{=}J$ or $J\pm 2ME_Z)\rightarrow 6p^2P_{\frac{3}{2},m_j}]$. Algebraic formula can be obtained by substituting Eqs. 4, 7, and 8, and the formulas in Table 1 of Ref. 15 into Eq. 9. The algebraic formulas of

$$\frac{1}{2J+1}\sum_{M=J}^{-J}P[^1\Sigma_g^+(v''J+1M)-{}^1\Sigma_u^+(vJM)-{}^3\Pi_{0u}(ev'JM)$$
$$-{}^3\Sigma_u^+(v_cN=J\text{ or }J\pm2ME_Z)\rightarrow 6p^2P_{\frac{3}{2},m_j}] \quad (10)$$

are listed in Table 1.

Discussion

By comparing the observed excitation spectra of the Cs-$(8s^2S_{\frac{1}{2},m_j'}\leftarrow 6p^2P_{\frac{3}{2},m_j})$ transitions (Figs. 3 and 4) and the calculated splittings and intensities (Fig. 5), we can assign the four lines from low to high energy as the $8s^2S_{\frac{1}{2},-\frac{1}{2}}\leftarrow 6p^2P_{\frac{3}{2},\frac{1}{2}}$, $8s^2S_{\frac{1}{2},\frac{1}{2}}\leftarrow 6p^2P_{\frac{3}{2},\frac{3}{2}}$, $8s^2S_{\frac{1}{2},-\frac{1}{2}}\leftarrow 6p^2P_{\frac{3}{2},-\frac{3}{2}}$, and $8s^2S_{\frac{1}{2},\frac{1}{2}}\leftarrow 6p^2P_{\frac{3}{2},-\frac{1}{2}}$ transitions. The observed intensity ratio

Table 1. Algebraic Formulas of $\sum_{M=J}^{-J} P[^1\Sigma_g^+ (v''J+1M)-{}^1\Sigma_u^+ (vJM)-{}^3\Pi_{0u} (ev'JM)-{}^3\Sigma_u^+ (v_cN=J \text{ or } J\pm 2ME_Z)-6p^2P_{\frac{3}{2},m_j}]/(2J+1)$ in Units of $\mu_\parallel^2\zeta^2 (J+1)/\{1260\pi(2J+1)\}$

E_Z	m_j	$\sum_{M=J}^{-J} P/(2J+1)$
$\pm 2\mu_B H$	$\pm\frac{3}{2}$	$C^2H^2(J+2)(28J^3+100J^2+129J+54)/\{8(2J+1)(2J+3)^3\}$
$\pm 2\mu_B H$	$\pm\frac{1}{2}$	$C^2H^2(J+2)(40J^3+148J^2+174J+81)/\{12(2J+1)(2J+3)^3\}$
$\pm 2\mu_B H$	$\mp\frac{1}{2}$	$C^2H^2(J+2)(28J^3+100J^2+129J+54)/\{24(2J+1)(2J+3)^3\}$
$\pm 2\mu_B H$	$\mp\frac{3}{2}$	0
0	$\pm\frac{3}{2}$	$C^2H^2(J+1)(J+2)(10J^2+21J+15)/\{4(2J+1)(2J+3)^3\}$
0	$\pm\frac{1}{2}$	$C^2H^2(J+2)(14J^3+49J^2+58J+27)/\{4(2J+1)(2J+3)^3\}$
$2\mu_B H$	$\frac{3}{2}$	$U^{a)}/\{8(2J-1)^2(2J+3)^3\}$
$-2\mu_B H$	$-\frac{3}{2}$	$V^{b)}/\{8(2J-1)^2(2J+3)^3\}$
$2\mu_B H$	$\frac{1}{2}$	$W^{c)}/\{12(2J-1)^2(2J+3)^3\}$
$-2\mu_B H$	$-\frac{1}{2}$	$X^{d)}/\{12(2J-1)^2(2J+3)^3\}$
$2\mu_B H$	$-\frac{1}{2}$	$U^{a)}/\{24(2J-1)^2(2J+3)^3\}$
$-2\mu_B H$	$\frac{1}{2}$	$V^{b)}/\{24(2J-1)^2(2J+3)^3\}$
$\pm 2\mu_B H$	$\mp\frac{3}{2}$	0
0	$\pm\frac{3}{2}$	$Y^{e)}/\{4(2J-1)^2(2J+3)^3\}$
0	$\pm\frac{1}{2}$	$Z^{f)}/\{4(2J-1)^2(2J+3)^3\}$
$\pm 2\mu_B H$	$\pm\frac{3}{2}$	$C^2H^2J(J-1)(7J-2)/\{4(2J+1)(2J-1)^2\}$
$\pm 2\mu_B H$	$\pm\frac{1}{2}$	$C^2H^2J(J-1)(5J-4)/\{3(2J+1)(2J-1)^2\}$
$\pm 2\mu_B H$	$\mp\frac{1}{2}$	$C^2H^2J(J-1)(7J-2)/\{12(2J+1)(2J-1)^2\}$
$\pm 2\mu_B H$	$\mp\frac{3}{2}$	0
0	$\pm\frac{3}{2}$	$C^2H^2J(J-1)(5J-1)/\{4(2J+1)(2J-1)^2\}$
0	$\pm\frac{1}{2}$	$C^2H^2J(J-1)(7J-5)/\{4(2J+1)(2J-1)^2\}$

a) $U=J\{C^2H^2(32J^4+124J^3+172J^2+23J-120)+42\sqrt{2}CHB_LJ(2J-1)(2J+3)^2+6B_L^2(2J-1)^2(2J+3)^2(16J^2+37J+24)\}$. b) $V=J\{C^2H^2(32J^4+124J^3+172J^2+23J-120)-42\sqrt{2}CHB_LJ(2J-1)(2J+3)^2+6B_L^2(2J-1)^2(2J+3)^2(16J^2+37J+24)\}$. c) $W=J\{C^2H^2(32J^4+112J^3+76J^2-16J+69)-42\sqrt{2}CHB_L(2J-1)(2J+3)^2+6B_L^2(2J-1)^2(2J+3)^2(24J^2+52J+15)\}$. d) $X=J\{C^2H^2(32J^4+112J^3+76J^2-16J+69)+42\sqrt{2}CHB_L(2J-1)(2J+3)^2+6B_L^2(2J-1)^2(2J+3)^2(24J^2+52J+15)\}$. e) $Y=\{2C^2H^2(100J^5+416J^4+413J^3-209J^2-279J+105)+3B_L^2J(2J+1)(2J-1)^2(2J+3)^2(5J+9)\}$. f) $Z=\{2C^2H^2(108J^5+392J^4+287J^3-265J^2-193J+105)+B_L^2J(2J+1)(2J-1)^2(2J+3)^2(13J+15)\}$.

is deviated from 1 : 3 : 3 : 1, which is the ratio of the squares of the transition moments. This indicates an anisotropic population on the magnetic sublevels $6p^2P_{\frac{3}{2},m_j}$. The Doppler profiles of the excitation spectra of the Cs($6p^2P_{\frac{3}{2},+\frac{3}{2}}$) and Cs($6p^2P_{\frac{3}{2},-\frac{3}{2}}$) atoms are similar, and those of the Cs($6p^2P_{\frac{3}{2},+\frac{1}{2}}$) and Cs($6p^2P_{\frac{3}{2},-\frac{1}{2}}$) atoms are also similar. However, those of the Cs($6p^2P_{\frac{3}{2},\pm\frac{3}{2}}$) atoms shown in Fig. 3, where the probe laser beam is propagated along the magnetic field with the σ-polarization, are different from those in Fig. 4, where the probe laser beam is propagated anti-parallel to the pump laser beam with the σ-polarization.

1. Doppler Profiles of Excitation Spectra of the Cs($6p^2P_{\frac{3}{2},m_j}$) Atoms. The Doppler profiles of the photofragments have been used to determine the angular anisotropy of the recoil velocities in photodissociation.[1—3,20—26] When the pump laser is polarized along the Z axis and the angular distribution of photofragments of fixed kinetic energy $\frac{1}{2}mv_0^2$ is measured by the probe laser propagated at an angle χ with the Z axis, the probability of finding the photofragments is given by[24,25]

$$P(\theta',\chi)=P_0[1+\beta P_2(\cos\theta')P_2(\cos\chi)], \tag{11}$$

where P_0 is a constant, β is the anisotropy parameter, $P_2(\cos\theta)$ is the second degree Legendre polynomial, and θ' is the angle between the propagation vector of the probe laser beam and the recoil velocity. This formula is valid when the recoil energy is large compared to the rotational energy, which is the case of this experiment. When the probe laser beam is propagated at right angles to the direction of the molecular beam, $\cos\theta'$ is given by

$$\cos\theta'=\left(\frac{c}{\nu_0\nu_r}\right)(\nu-\nu_0), \tag{12}$$

where ν_0 is the frequency which would be absorbed by molecules at a stand, v_r is the recoil velocity, and c is the speed of light. When the probe laser beam is propagated along the Z axis, $\chi=0$, the Doppler line profile is given by

$$P(\nu) = P_0\left[1+\frac{\beta}{2}\left\{3\left(\frac{c}{\nu_0 v_r}\right)^2(\nu-\nu_0)^2-1\right\}\right]. \quad (13)$$

When the probe laser beam is propagated anti-parallel to the pump laser beam, $\chi=\pi/2$, the Doppler line profile is given by

$$P(\nu) = P_0\left[1-\frac{\beta}{4}\left\{3\left(\frac{c}{\nu_0 v_r}\right)^2(\nu-\nu_0)^2-1\right\}\right]. \quad (14)$$

The energy of the $Cs_2D^1\Sigma_u^+$ (v=46, J=54) molecule is redistributed to the dissociated atoms $Cs(6s^2S_{\frac{1}{2},m_j})$ and $Cs(6p^2P_{\frac{3}{2},m_j})$. If we neglect the small energy of the Zeeman interaction, the magnitude of the recoil velocity v_r is evaluated to be 435 m s^{-1} from the relation

$$\frac{1}{2}m_{Cs}v_r^2 = \frac{1}{2}\{E[D^1\Sigma_u^+(v=46,J=54)] - E[6p^2P_{\frac{3}{2}}+6s^2S_{\frac{1}{2}}]\}, \quad (15)$$

where m_{Cs} is the mass of a ^{133}Cs atom, $E[D^1\Sigma_u^+(v$=46, J=54)] is the term value of the $D^1\Sigma_u^+(v$=46, J=54) level, and $E[6p^2P_{\frac{3}{2}}+6s^2S_{\frac{1}{2}}]$ is the electronic energy of the dissociated atoms $Cs(6p^2P_{\frac{3}{2}})$ and $Cs(6s^2S_{\frac{1}{2}})$.

When we analyze the excitation spectrum of the photodissociated $Cs(6p^2P_{\frac{3}{2}})$ atom, we have to take into account the fact that a large number of $Cs(6s^2S_{\frac{1}{2}})$ atoms coexist within the molecular beam of Cs_2; the ratio of Cs to Cs_2 is about 10^2. The $Cs(6p^2P_{\frac{3}{2}} \rightarrow 6s^2S_{\frac{1}{2}})$ emission (D_2 line) can be absorbed by the $Cs(6s^2S_{\frac{1}{2}})$ atoms in the molecular beam. This is called self-absorption. The $Cs(6p^2P_{\frac{3}{2}})$ atoms produced by the self-absorption can also be excited by the probe laser beam. Since the velocity vectors of these atoms are aligned along the propagation vector of the molecular beam, the linewidth of the excitation spectrum of these atoms can be estimated to be about 30 MHz (FWHM), which is the residual Doppler width in our experimental setup. The linewidth due to lifetime broadening is evaluated to be 1.7 MHz (FWHM) from the reported lifetime 95 ns of the Cs $8s^2S_{\frac{1}{2}}$ state,[27] and therefore can be neglected. We evaluated the m_j dependence of population and the effect of self-absorption by simulating the observed spectra. The line positions and the transition probabilities are assumed to be the same with those in Fig. 5, and the lineshape of each transition is expressed by the Gaussian function of the linewidth 30 MHz (FWHM). The relative intensity of the transition induced by self-absorption to the one in the absence of self-absorption was fit to the observed excitation spectra. The results are shown in Figs. 3 and 4.

The Doppler line profile of a transition to each hyperfine component for the probe beam propagated along the Z axis is given by Eq. 13, and that for the probe beam propagated anti-parallel to the pump beam is given by Eq. 14. The line profile of each Zeeman component was simulated by the superposition. By a least-squares fitting to reproduce the Doppler line profiles, we determined the anisotropy parameters to be $\beta=-0.86$ for $m_j=\pm\frac{3}{2}$ and $\beta=0.45$ for $m_j=\pm\frac{1}{2}$. The resulting line profiles are shown in Figs. 3(b) and 4(b); the solid lines show the spectra without self-absorption, and the broken lines show the spectra including the effect of self-absorption. The angular distribution of the recoil velocity v_r pumped by a laser beam polarized along the Z axis is given by[3] $1+\beta P_2(\cos\theta)$, where θ is the angle between the recoil velocity and the Z axis, which is coincident with the direction of the magnetic field $\boldsymbol{H}$. The values of $1-0.86P_2(\cos\theta)$ for $Cs(6p^2P_{\frac{3}{2},\pm\frac{3}{2}})$ and $1+0.45P_2(\cos\theta)$ for $Cs(6p^2P_{\frac{3}{2},\pm\frac{1}{2}})$ are plotted against θ in Fig. 6. It shows that the $Cs(6p^2P_{\frac{3}{2},\pm\frac{1}{2}})$ atoms recoil predominantly parallel to $\boldsymbol{H}$ and the $Cs(6p^2P_{\frac{3}{2},\pm\frac{3}{2}})$ atoms recoil predominantly perpendicular to $\boldsymbol{H}$.

If we express the eigenfunction of the atomic state by basis functions $|Lm_L>|Sm_S>$, where $|Lm_L>$ and $|Sm_S>$ are, respectively, the orbital part and the spin part, the wave functions of the $^2P_{\frac{3}{2},\pm\frac{3}{2}}$ and $^2P_{\frac{3}{2},\pm\frac{1}{2}}$ states are, respectively, given by $|1\pm1>|\frac{1}{2}\pm\frac{1}{2}>$ and $\sqrt{\frac{1}{3}}|1\pm1>|\frac{1}{2}\mp\frac{1}{2}>+\sqrt{\frac{2}{3}}|10>|\frac{1}{2}\pm\frac{1}{2}>$. When the $Cs(6p^2P_{\frac{3}{2},\pm\frac{3}{2}})$ atom recoils perpendicular to $\boldsymbol{H}$, the 6p orbital is directed predominantly perpendicular to $\boldsymbol{H}$. When the $Cs(6p^2P_{\frac{3}{2},\pm\frac{1}{2}})$ atom recoils parallel to $\boldsymbol{H}$, the 6p orbital is directed predominantly parallel to $\boldsymbol{H}$. These are shown

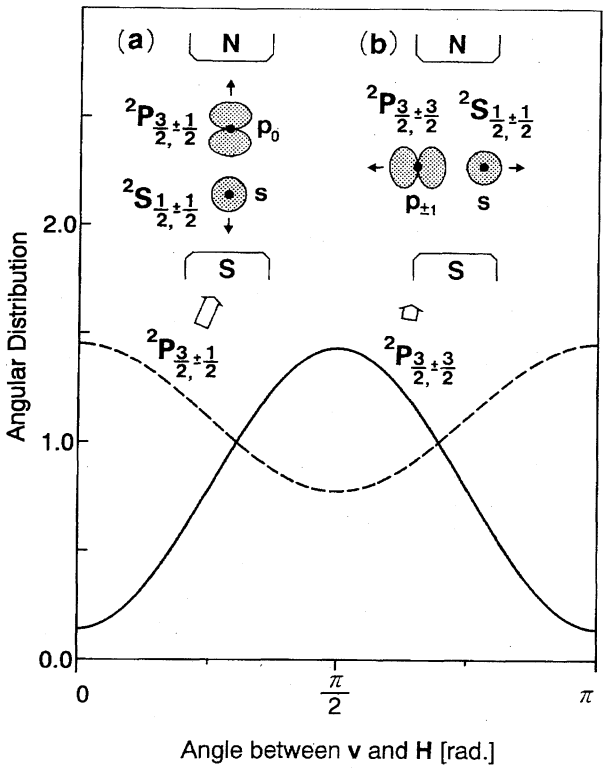

Fig. 6. Angular distribution of the recoil velocity of the $Cs(6p^2P_{\frac{3}{2},\pm\frac{3}{2}})$ and $Cs(6p^2P_{\frac{3}{2},\pm\frac{1}{2}})$ atoms are respectively shown by a full line and a broken line as a function of angle between the recoil velocity and the magnetic field. In the upper area, the recoil velocity and the orientation of the 6p orbital of the dissociating $Cs(6p^2P_{\frac{3}{2},m_j})$ atom is illustrated. (a) In case the $Cs(6p^2P_{\frac{3}{2},\pm\frac{1}{2}})$ atom recoils parallel to $\boldsymbol{H}$. (b) In case the $Cs(6p^2P_{\frac{3}{2},\pm\frac{3}{2}})$ atom recoils perpendicular to $\boldsymbol{H}$.

schematically in Fig. 6; it seems reasonable because the Cs_2 molecule excited to the $D^1\Sigma_u^+$ state dissociates through the $^3\Sigma_u^+$ state, and therefore the 6p orbital is directed along the molecular axis.

2. Population Analysis. For the $8s^2S_{\frac{1}{2},\frac{1}{2}} \leftarrow 6p^2P_{\frac{3}{2},\frac{3}{2}}$, $8s^2S_{\frac{1}{2},-\frac{1}{2}} \leftarrow 6p^2P_{\frac{3}{2},\frac{1}{2}}$, $8s^2S_{\frac{1}{2},\frac{1}{2}} \leftarrow 6p^2P_{\frac{3}{2},-\frac{1}{2}}$, and $8s^2S_{\frac{1}{2},-\frac{1}{2}} \leftarrow 6p^2P_{\frac{3}{2},-\frac{3}{2}}$ transitions, the line intensities were observed to be in the ratio of 234 : 139 : 100 : 136 in the spectrum shown in Fig. 3(a), and 229 : 132 : 100 : 138 in the spectrum shown in Fig. 4(a). The line intensity is proportional to the product of the population of the $Cs(6p^2P_{\frac{3}{2},m_j})$ atoms and the probability of the $8s^2S_{\frac{1}{2},m_j'} \leftarrow 6p^2P_{\frac{3}{2},m_j}$ transition. The transition probabilities of the $8s^2S_{\frac{1}{2},\frac{1}{2}} \leftarrow 6p^2P_{\frac{3}{2},\frac{3}{2}}$, $8s^2S_{\frac{1}{2},-\frac{1}{2}} \leftarrow 6p^2P_{\frac{3}{2},\frac{1}{2}}$, $8s^2S_{\frac{1}{2},\frac{1}{2}} \leftarrow 6p^2P_{\frac{3}{2},-\frac{1}{2}}$, and $8s^2S_{\frac{1}{2},-\frac{1}{2}} \leftarrow 6p^2P_{\frac{3}{2},-\frac{3}{2}}$ transitions are in the ratio of 3 : 1 : 1 : 3 for the σ-polarization. Therefore, the ratio of the population of the $Cs(6p^2P_{\frac{3}{2},m_j})$ atoms to $m_j=\frac{3}{2},\frac{1}{2},-\frac{1}{2},-\frac{3}{2}$ was evaluated to be 78 : 139 : 100 : 45 from the spectrum in Fig. 3(a), and 76 : 132 : 100 : 46 from the spectrum in Fig. 4(a); the average is in the ratio of 77 : 136 : 100 : 46.

The population ratio of the $Cs(6p^2P_{\frac{3}{2},m_j})$ atoms produced by the predissociation following the $D^1\Sigma_u^+(v=46, J=54) \leftarrow X^1\Sigma_g^+(v=0, J=55)$ excitation can be calculated by the algebraic formulas in Table 1 and it depends on the ratio of B_L to CH. The ratio $B_L : CH$ may be evaluated by $\frac{\hbar^2}{2\mu R_c^2} : \frac{\mu_B H}{\sqrt{2}}$, where R_c is the internuclear distance at the crossing point of the potential curves of the $(2)^3\Pi_{0u}$ and $c^3\Sigma_u^+$ states. The R_c is estimated to be 12 a_0 from ab initio MO calculation,[28] where a_0 is the Bohr radius. The ratio $B_L : CH$ is evaluated to be 1 : 10 for H=1.91 kG and R_c=12 a_0. Calculated ratios of the $Cs(6p^2P_{\frac{3}{2},m_j})$ atoms for H=0, $B_L : CH$=1 : 10, and $B_L : CH$=1 : 50 are listed in Table 2. From the results, we can see that the effects of the interaction between the $(2)^3\Pi_{0u}(ev'J=54)$ and $c^3\Sigma_u^+$ (v_cN=52 or 56 E_Z) levels are small, and can be neglected at H=1.91 kG. The predissociation increases significantly at $B_L : CH$=1 : 50 only through the $c^3\Sigma_u^+(v_cN=54\ E_Z=0)$ level. If we assume that the predissociation occurs independent of E_Z, the population to the $Cs(6p^2P_{\frac{3}{2},m_j})$ levels were calculated to be in the ratio of 82 : 100 : 100 : 82 for $m_j=\frac{3}{2},\frac{1}{2},-\frac{1}{2}$, and $-\frac{3}{2}$. This result is coincident with the experimental result that the $Cs(6p^2P_{\frac{3}{2},\pm\frac{1}{2}})$ levels are more preferentially populated than the $Cs(6p^2P_{\frac{3}{2},\pm\frac{3}{2}})$ levels. However, this calculation cannot reproduce the observed results that the $Cs(6p^2P_{\frac{3}{2},\frac{1}{2}})$ level is more preferentially populated than the $Cs(6p^2P_{\frac{3}{2},-\frac{1}{2}})$ level and the $Cs(6p^2P_{\frac{3}{2},\frac{3}{2}})$ level is more preferentially populated than the $Cs(6p^2P_{\frac{3}{2},-\frac{3}{2}})$ level.

The overlap integral $<v'|v_c>$ depends on the Zeeman energy E_Z, and can be sensitive to the level energy near to the potential crossing. If the potential curve of the $c^3\Sigma_u^+(v_cNE_Z)$ state has a gradient of $-100\ cm^{-1}/Å$ around the intersection with the potential curve of the $(2)^3\Pi_{0u}(ev'J)$ state, the vibrational wave function $|v_c$ of $c^3\Sigma_u^+(v_cN=54\ E_Z=0)>$ is shifted toward the long internuclear distance by 0.002 Å from the vibrational wave function $|v_c$ of $c^3\Sigma_u^+(v_cN=54\ E_Z=2\mu_BH)>$ at H=1.91 kG. The magnitude of the overlap integral $<v'|v_c>$ may change considerably with this amount of shift. If the overlap integrals of vibrational wave functions $<v'$ of $(2)^3\Pi_{0u}(ev'J=54M)|v_c$ of $c^3\Sigma_u^+(v_cN=54\ E_Z=2\mu_BH)>$, $<v'$ of $(2)^3\Pi_{0u}(ev'J=54M)|v_c$ of $c^3\Sigma_u^+(v_cN=54\ E_Z=0)>$, and $<v'$ of $(2)^3\Pi_{0u}(ev'J=54M)|v_c$ of $c^3\Sigma_u^+(v_cN=54\ E_Z=-2\mu_BH)>$ are in the ratio of about 7 : 6 : 5, the population ratio between $6p^2P_{\frac{3}{2},\frac{3}{2}}$, $6p^2P_{\frac{3}{2},\frac{1}{2}}$, $6p^2P_{\frac{3}{2},-\frac{1}{2}}$, and $6p^2P_{\frac{3}{2},-\frac{3}{2}}$ is calculated to be 118 : 131 : 107 : 71. This result is in agreement with the observed population ratio of 77 : 46 between the $6p^2P_{\frac{3}{2},\frac{3}{2}}$ and $6p^2P_{\frac{3}{2},-\frac{3}{2}}$ levels and the ratio 139 : 100 between the $6p^2P_{\frac{3}{2},\frac{1}{2}}$ and $6p^2P_{\frac{3}{2},-\frac{1}{2}}$ levels. However, the observed population ratio of the $6p^2P_{\frac{3}{2},\pm\frac{3}{2}}$ levels to the $6p^2P_{\frac{3}{2},\pm\frac{1}{2}}$ levels is about 2/3 of the calculated one. The present theoretical analysis on the M dependence of the predissociation can not explain this discrepancy, because the dissociation rate is symmetric

Table 2. Ratio of the Values of $\sum_{M=54}^{-54} P[^1\Sigma_g^+(v''55M) - {}^1\Sigma_u^+(v54M) - {}^3\Pi_{0u}(ev'54M) - {}^3\Sigma_u^+(v_cN=54 \text{ or } 54 \pm 2ME_Z) \rightarrow 6p^2P_{\frac{3}{2},m_j}]/109$ for H=0, $B_L : CH$=1 : 10, and $B_L : CH$= 1 : 50

	N	E_Z	m_j=	$\frac{3}{2}$	$\frac{1}{2}$	$-\frac{1}{2}$	$-\frac{3}{2}$
H= 0	56	$+2\mu_BH$		0	0	0	0
	56	0		0	0	0	0
	56	$-2\mu_BH$		0	0	0	0
	54	$+2\mu_BH$		453	452	151	0
	54	0		145	124	124	145
	54	$-2\mu_BH$		0	151	452	453
	52	$+2\mu_BH$		0	0	0	0
	52	0		0	0	0	0
	52	$-2\mu_BH$		0	0	0	0
		Total		598	727	727	598
B_L:CH = 1 : 10	56	$+2\mu_BH$		1	1	0	0
	56	0		0	1	1	0
	56	$-2\mu_BH$		0	0	1	1
	54	$+2\mu_BH$		454	452	151	0
	54	0		149	129	129	149
	54	$-2\mu_BH$		0	151	452	453
	52	$+2\mu_BH$		1	1	0	0
	52	0		0	1	1	0
	52	$-2\mu_BH$		0	0	1	1
		Total		605	736	736	604
B_L:CH = 1 : 50	56	$+2\mu_BH$		14	13	5	0
	56	0		10	14	14	10
	56	$-2\mu_BH$		0	5	13	14
	54	$+2\mu_BH$		463	457	154	0
	54	0		246	232	232	246
	54	$-2\mu_BH$		0	153	457	459
	52	$+2\mu_BH$		14	13	5	0
	52	0		10	14	14	10
	52	$-2\mu_BH$		0	5	13	14
		Total		757	906	907	753

with respect to M, as we can see from the algebraic formula of $P[^1\Sigma_g^+(v''J+1M)-^1\Sigma_u^+(vJM)-^3\Pi_{0u}(ev'JM)-^3\Sigma_u^+(v_cN=J$ or $J\pm2ME_Z)-6p^2P_{\frac{3}{2},m_j}]$. More extensive studies are necessary to solve this discrepancy.

The authors are grateful to Dr. S. Kasahara, Y. Hasui, and T. Kokita for their help in the experimental work. This work was supported by a grant in aid for specially promoted research from the Ministry of Education, Science and Culture. K. M. wishes to express his thanks for Fellowships of the Japan Society for the Promotion of Science for Japanese Junior Scientists.

References

1) G. E. Hall and P. L. Houston, *Annu. Rev. Phys. Chem.*, **40**, 375 (1989).
2) "Molecular Photodissociation Dynamics," ed by M. N. R. Ashfold and J. E. Baggott, Roy. Soc. Chem., London (1987).
3) R. N. Zare and D. R. Herschbach, *Proc. IEEE*, **51**, 173 (1963).
4) R. J. Van Brunt and R. N. Zare, *J. Chem. Phys.*, **48**, 4304 (1968).
5) H. Katô and M. Baba, *Chem. Rev.*, **95**, 2311 (1995).
6) C. B. Collins, F. W. Lee, J. A. Anderson, P. A. Vicharelli, D. Popescu, and I. Popescu, *J. Chem. Phys.*, **74**, 1067 (1981).
7) M. Raab, G. Höning, W. Demtröder, and C. R. Vidal, *J. Chem. Phys.*, **76**, 4370 (1982).
8) C. Amiot, W. Demtröder, and C. R. Vidal, *J. Chem. Phys.*, **88**, 5265 (1988).
9) H. Katô, T. Kobayashi, M. Chosa, T. Nakahori, T. Iida, S. Kasahara, and M. Baba, *J. Chem. Phys.*, **94**, 2600 (1991).
10) H. Katô, T. Kobayashi, Y. C. Wang, K. Ishikawa, M. Baba, and S. Nagakura, *Chem. Phys.*, **162**, 107 (1992).
11) H. Katô, T. Kumauchi, K. Nishizawa, M. Baba, and K. Ishikawa, *J. Chem. Phys.*, **98**, 6684 (1993).
12) E. Arimondo, M. Inguscio, and P. Violino, *Rev. Mod. Phys.*, **49**, 31 (1977).
13) A. Corney, "Atomic and Laser Spectroscopy," Oxford University Press, Oxford (1977).
14) E. U. Condon and G. H. Shortley, "The Theory of Atomic Spectra," Cambridge University Press, Cambridge (1951).
15) H. Katô and K. Onomichi, *J. Chem. Phys.*, **82**, 1642 (1985).
16) H. Katô, *Bull. Chem. Soc. Jpn.*, **66**, 3203 (1993).
17) E. Wigner and E. E. Witmer, *Z. Phys.*, **51**, 859 (1928).
18) R. S. Mulliken, *Phys. Rev.*, **36**, 1440 (1930).
19) S. J. Singer, K. F. Freed, and Y. B. Band, *J. Chem. Phys.*, **79**, 6060 (1983).
20) C. Jonah, *J. Chem. Phys.*, **55**, 1915 (1971).
21) R. N. Zare, *Mol. Photochem.*, **4**, 1 (1972).
22) S-C. Yang and R. Bersohn, *J. Chem. Phys.*, **61**, 4400 (1974).
23) J. L. Kinsery, *J. Chem. Phys.*, **66**, 2560 (1977).
24) R. Schmiedl, H. Dugan, W. Meier, and K. H. Welge, *Z. Phys. A*, **304**, 137 (1982).
25) R. N. Dixon, *J. Chem. Phys.*, **85**, 1866 (1986).
26) G. E. Hall, N. Sivakumar, P. L. Houston, and I. Burak, *Phys. Rev. Lett.*, **56**, 1671 (1986).
27) A. A. Radzig and B. M. Smirnov, "Reference Data on Atoms, Molecules, and Ions," Springer, Berlin (1985).
28) N. Spiess, Ph. D. Thesis, Fachbereich Chemie, Universität Kaiserslautern, 1989.